Molecular Crystals and Liquid Crystals Science and Technology. Section A. Molecular Crystals and Liquid Crystals
Publication details, including instructions for authors and subscription information:
http://www.tandfonline.com/loi/gmcl19

Rheological Behavior of Thermotropic Liquid-Crystalline Polymers: Effects of Thermal and Deformation Histories

Chang Dae Han [a] , Sukky Chang [a] & Seung Su Kim [a]
[a] Department of Polymer Engineering and Institute of Polymer Engineering, The University of Akron, Akron, Ohio, 44325-0301, U.S.A.
Version of record first published: 24 Sep 2006.

To cite this article: Chang Dae Han , Sukky Chang & Seung Su Kim (1994): Rheological Behavior of Thermotropic Liquid-Crystalline Polymers: Effects of Thermal and Deformation Histories, Molecular Crystals and Liquid Crystals Science and Technology. Section A. Molecular Crystals and Liquid Crystals, 254:1, 335-368

To link to this article: http://dx.doi.org/10.1080/10587259408036085

Mol. Cryst. Liq. Cryst. 1994, Vol. 254, pp. 335–368
Reprints available directly from the publisher
Photocopying permitted by license only

Printed in the United States of America

RHEOLOGICAL BEHAVIOR OF THERMOTROPIC LIQUID-CRYSTALLINE POLYMERS: EFFECTS OF THERMAL AND DEFORMATION HISTORIES

CHANG DAE HAN, SUKKY CHANG AND SEUNG SU KIM
Department of Polymer Engineering and Institute of Polymer Engineering,
The University of Akron, Akron, Ohio 44325-0301, U.S.A.

(Received: February 7, 1994)

Abstract The effects of thermal and deformation histories on the rheological behavior of thermotropic liquid-crystalline polymers (TLCPs) were investigated using a cone-and-plate rheometer. For the study, two TLCPs were used: (1) the copolyester consisting of 73 mol % hydroxybenzoic acid (HBA) and 27 mol % 6-hydroxy-2-naphthoic acid (HNA) (Vectra A900) having the clearing temperature (T_{cl}) close to or above thermal degradation temperature (ca. 350 °C) and (2) an aromatic polyester, poly[(phenylsulfonyl)-*p*-phenylene 1,10-decamethylene-bis(4-oxybenzoate)] (PSHQ10) having a T_{cl} of 175 °C, which was synthesized in our laboratory. In the use of PSHQ10, we were able to control the initial conditions of the specimens before being subjected to shear flow in the nematic region by first heating a solvent-cast specimen to the isotropic state and then cooling slowly to the nematic region. This was not possible, however, for Vectra A900. We found that the first normal stress difference (N_1) of PSHQ10 in the *nematic* state is *positive* at shear rates ($\dot{\gamma}$) of 0.008-1.08 s^{-1} tested, and that values of N_1 for Vectra A900 are also *positive* at $\dot{\gamma}$ = 0.01-1.0 s^{-1} tested when using, as a reference state, the *true* zero value of normal stress that existed before the sample loading began.

INTRODUCTION

Over the past decade, a number of research groups reported on the rheological behavior of thermotropic liquid-crystalline polymers (TLCPs).[1-19] Of particular interest is the experimental observation that the rheological behavior of TLCPs is very sensitive to thermal and deformation histories,[16] which is not the case for flexible homopolymers.

Therefore, unless the thermal and deformation histories of a TLCP are kept identical, the rheological measurements made by one research group can be different from those made by another research group.

Owing to the rather complicated relationships existing between the rheological behavior and the domain texture in TLCPs, before taking rheological measurements one must be able to control the initial morphology (i.e., initial conditions) of the specimens; otherwise, it would not be possible for one to separate the effect of test temperature and the effect of thermal history from the overall rheological responses.

In this paper we shall report on the results of our recent rheological investigation on a liquid-crystalline thermotropic copolyester consisting of hydroxybenzoic acid (HBA) and 6-hydroxy-2-naphthoic acid (HNA) and an aromatic polyester that was synthesized in our laboratory. In this study, emphasis was placed on investigating the effects of thermal and deformation histories on the transient, steady-state and oscillatory shear flow behavior of these TLCPs. We shall point out, as noted earlier by Cocchini et al.,[11,20] that in the use of Vectra A900 a substantial amount of normal stress, which is introduced by the squeeze flow during sample loading, may be present in the specimen, which decays very slowly with time. Thus, the presence of the *unrelaxed* normal stress in the specimen can lead one to erroneously interpret values of N_1 to be *negative* at low shear rates below a certain critical value *if* the *unrelaxed* normal stress values were assumed to be the *true* zero value of the normal stress.

EXPERIMENTAL

Materials

In the present study, a thermotropic liquid-crystalline polyester, poly[(phenylsulfonyl)-*p*-phenylene 1,10-decamethylene-bis(4-oxybenzoate)] (PSHQ10) was synthesized. The details of the procedures for synthesizing PSHQ10 are given by Furukawa and Lenz[21] and Kim and Han.[18] The chemical structure of PSHQ10 with the repeat unit

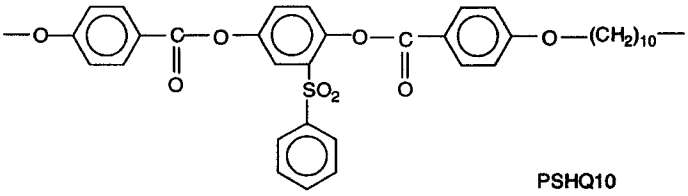

PSHQ10

was confirmed via 2-dimensional high-resolution nuclear magnetic resonance spectroscopy.[18] In the present study PSHQ10s having two different molecular weights were used, namely, one (PSHQ10-A) having the weight average molecular weight (M_w) of 46,000, and the other (PSHQ10-B) having M_w of 52,000, relative to polystyrene standards as determined by gel permeation chromatography.

Also employed in this study was the copolyester of 73 mol % hydroxybenzoic acid (HBA) and 27 mol % 6-hydroxy-2-naphthoic acid (HNA) (Vectra A900, Hoechst-Celanese Co.).

Sample Preparation

Vectra A900 specimens for rheological measurements were prepared by compression molding at 320 °C under vacuum into disks (the diameter of 20 mm and the thickness of 1 or 2 mm) and then cooled slowly to room temperature. PSHQ10 specimens for rheological measurements were prepared by first dissolving PSHQ10 in dichloromethane in the presence of an antioxidant (Irganox 1010, Ciba-Geigy Group) and then slowly evaporating the solvent at room temperature for a week. The cast films with the thickness of about 1 mm were further dried in a vacuum oven (30 mm Hg) at room temperature for at least 3 weeks and at 90 °C for 48 h. Right before the rheological measurement, specimens of PSHQ10 were further dried at 120 °C under vacuum to remove any residual solvent and moisture, and specimens of Vectra A900 were further dried at 120 °C under vacuum for 6-10 h to remove any moisture.

Differential Scanning Calorimetry

Thermal transition temperatures of the TLCPs employed were determined by differential scanning calorimetry (DSC) (Perkin-Elmer DSC-7). All DSC runs were made under a nitrogen atmosphere with heating and cooling rates of 20 °C/min. PSHQ10 was found to have (a) the glass transition temperature of 88°C, (b) a melting point (T_m) of 115 °C, and a nematic-to-isotropic transition temperature (T_{NI}) of 175 °C. Vectra A900 was found to have a T_m of 285 °C and a clearing temperature very close to or above thermal degradation temperatures (ca. 350 °C).

Rheological Measurement

In the rheological measurements for Vectra A900 and PSHQ10-B, a Rheometrics mechanical spectrometer (RMS Model 800) was used. The cone-and-plate (25 mm diameter plate and 0.1 radians cone angle) configuration was used to measure, (a) in the

transient shear mode, the shear stress growth ($\sigma^+(t,\dot{\gamma})$) and first normal stress difference growth ($N_1^+(t,\dot{\gamma})$) as functions of time (t) for various shear rates ($\dot{\gamma}$) and temperatures, and (b) in the steady-state shear mode, shear viscosity (η) and first normal stress difference (N_1) as functions of shear rate ($\dot{\gamma}$) and temperature. The Rheometrics RMS 800 was also used in the parallel-plate configuration to measure, in the oscillatory shear mode, the dynamic storage modulus (G') and dynamic loss modulus (G") as functions of angular frequency (ω) for various temperatures. From the measurements of G' and G", the absolute values of complex viscosity $|\eta^*(\omega)|$ were calculated using the relationship: $|\eta^*(\omega)| = [(G'(\omega)/\omega)^2 + (G''(\omega)/\omega)^2]^{0.5}$. In the oscillatory measurements, strain amplitude was varied from 0.01 to 0.06, which was well within the linear viscoelastic range of the materials investigated.

In the rheological measurements for PSHQ10-A, a Weissenberg rheogoniometer (Model R16, Sangamo Control) in the cone-and-plate (25 mm diameter plate and 0.07 radians cone angle) configuration was used in the transient and oscillatory shear modes. All experiments were conducted in the presence of nitrogen in order to preclude oxidative degradation of the specimen. Temperature control was satisfactory to within ±1 °C. The gap setting used in the cone-and-plate configuration was 50 μm for Vectra A900, and 160 μm for PSHQ10. The larger gap setting used for the PSHQ10 specimens was due to the fact that the viscosities of PSHQ10 were about an order of magnitude greater than those of Vectra A900, and thus it was difficult to adjust the gap setting as small as 50 μm.

RESULTS AND DISCUSSION

Effect of Thermal History on the Oscillatory Shear Flow Behavior

Vectra A900. Figure 1 gives variations of G' and G" with time for Vectra A900 at 290 °C, having two different thermal histories, namely, (○, ●) the specimen that was placed in the cone-and-plate fixture preheated to 290 °C and (△, ▲) the specimen that was first heated to 320 °C for 1 min and then cooled down to 290 °C. Figure 1 was obtained using a strain amplitude of 0.05 and an angular frequency (ω) of 1 rad/s. It can be seen in Figure 1 that preheating a specimen at 320 °C for 1 min gives rise to constant values of G' and G" at 290 °C for about 60 min, whereas values of G' and G" for the specimen which did not receive thermal treatment at 320 °C increase rapidly with time from the onset. These observations are consistent with the earlier findings of Lin and

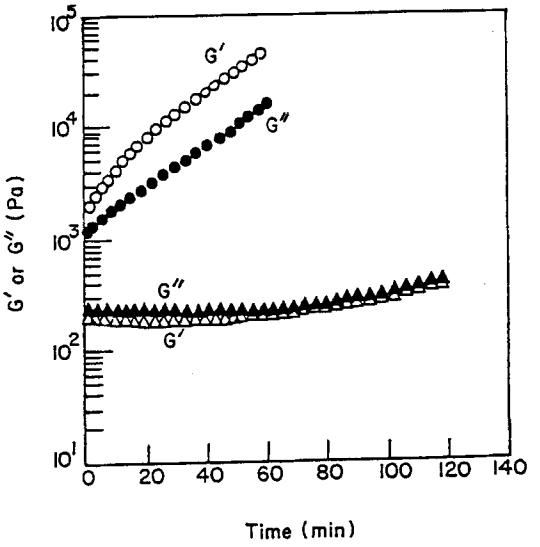

FIGURE 1 Variations of G' (O) and G" (●) with time for a Vectra A900 specimen placed in the cone-and-plate fixture at 290 °C and then annealed there for 1 h; and variations of G' (Δ) and G" (▲) with time for a Vectra A900 specimen, which was placed in the cone-and-plate fixture at 290 °C, heated to 320 °C for 1 min, and then cooled down to 290 °C followed by annealing for 2 h. Small amplitude oscillatory deformations with strain amplitude of 0.05 and angular frequency of 1 rad/s were applied to the specimens.

Winter,[22] who speculated that the 'residual' HBA in Vectra A900 melted away at ca. 320 °C and thus the specimen which received thermal treatment at 320 °C was stable at 290 °C for about 60 min.

The morphology of Vectra A900 is indeed very complex.[23,24] Figure 2 gives traces of DSC at heating and cooling rates of 20 °C/min. It can be seen in Figure 2 that Vectra A900 has a melting point of about 285 °C and does not show the clearing temperature even when heated to ca. 350 °C. It is of interest to further observe in Figure 3 that the annealing temperature affects the thermal transition behavior of Vectra A900, namely, when annealed at 280 °C for 50 min, an additional endothermic peak appears at 305 °C, which then is increased to 309 °C when annealed at 285 °C for 50 min. It is not clear to us what this structure is, which appeared on the DSC trace when Vectra A900 was annealed at temperatures below its nominal melting point.

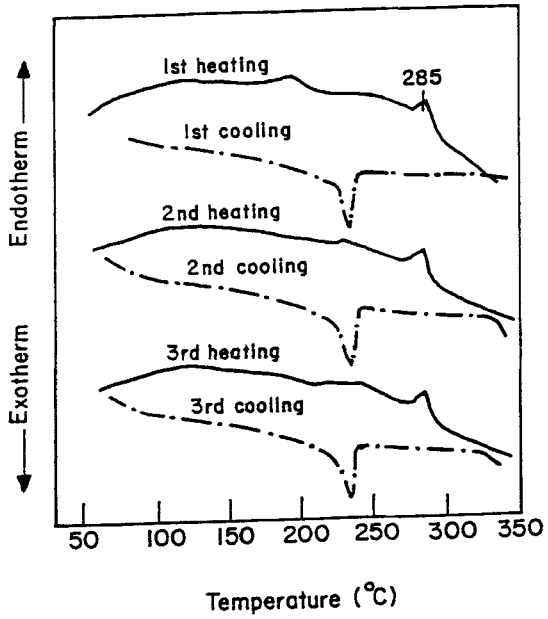

FIGURE 2 DSC traces for Vectra A900 specimens at various heating and cooling cycles at 20 °C/min.

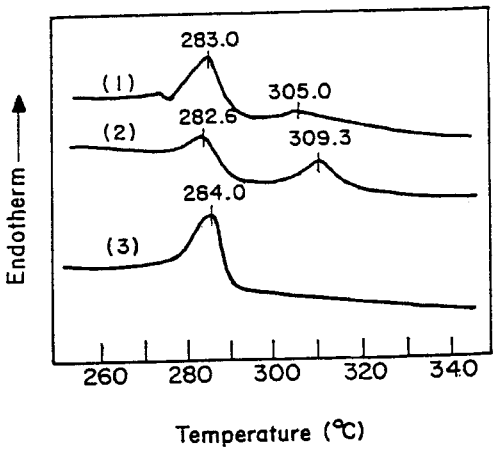

FIGURE 3 DSC traces for Vectra A900 specimens annealed at different temperatures: curve 1 annealed at 280 °C for 50 min; curve 2 annealed at 285 °C for 50 min; curve 3 annealed at 290 °C for 50 min.

Figure 4 gives variations of G' and G" with time for Vectra A900 at 320 °C, for the specimen which was placed in the cone-and-plate fixture of the RMS 800 that had been preheated to 320 °C. In obtaining the results given in Figure 4, a strain amplitude of 0.05 and an angular frequency of 1 rad/s were used. It can be seen in Figure 4 that values of G' and G" are more or less constant for about 10 min after the specimen was placed in the cone-and-plate fixture and then increase rapidly. This observation is consistent with that made earlier by Cocchini et al.,[11] who speculated that the observed increase in G' and G" at 320 °C may be attributable to post polymerization. What is not clear to us is the reason(s) why post polymerization, if it occurs, starts about 10 min after sample loading in the cone-and-plate fixture.

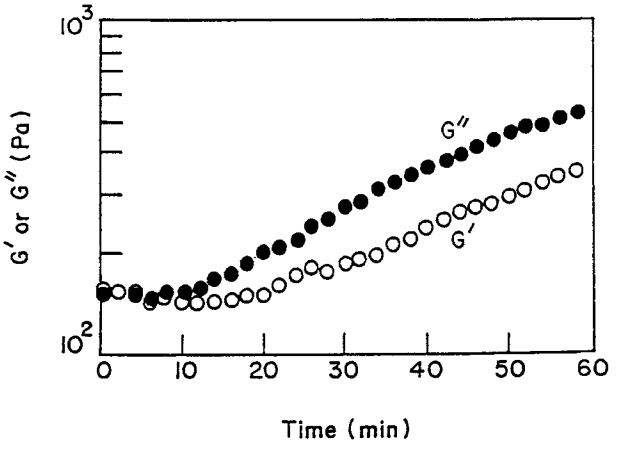

FIGURE 4 Variations of G' (○) and G" (●) with time for a Vectra A900 specimen placed in the cone-and-plate fixture at 320 °C and annealed there.

Figure 5 describes the effect of thermal history on the frequency dependence of G' and complex viscosity $|\eta^*|$ for Vectra A900. Also given in Figure 5 is the temperature protocol employed in obtaining the rheological data. In this experiment, a specimen was loaded in the cone-and-plate fixture at 290 °C which took about 10 min and then a frequency sweep was conducted at 290 and 320 °C, respectively, as indicated in the temperature protocol described in Figure 5. The following observations are worth noting in Figure 5: (1) values of G' and $|\eta^*|$ in step (3) (Δ) do not overlap those in step 5 (▲), although rheological measurements were taken at 290 °C; and (2) values of G' and $|\eta^*|$ in step (2) (○) do not overlap those in step 4 (●), although rheological

measurements were taken at 320 °C. This can be explained with the aid of Figure 1 in that, values of G' and $|\eta^*|$ at 290 °C would be more or less constant only for about 1 h, whereas the entire experiment described in Figure 5 lasted about 2 h. In other words, due to the morphological change occurring in Vectra A900, the rheological data could not be reproduced at 290 and 320 °C, respectively, for a period of 2 h.

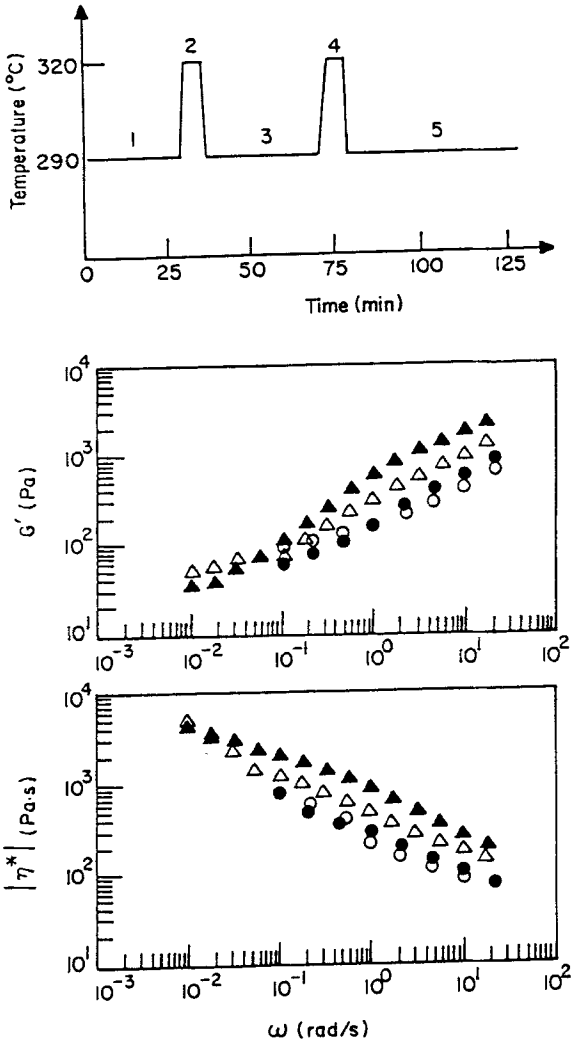

FIGURE 5 Temperature protocols employed, and plots of log G' and log $|\eta^*|$ versus log ω for a Vectra A900 specimen having the thermal histories as indicated in the temperature protocol: (O) step 2; (Δ) step 3; (●) step 4; (▲) step 5.

Figure 6 gives plots of log G' versus log G" for Vectra A900, which were obtained using the plots given in Figure 5. According to Han and coworkers,[17,18,25-30] log G' versus log G" plots are very sensitive to the morphological state of a multiphase polymer (e.g., microphase-separated block copolymers; liquid-crystalline polymers in an *anisotropic* state) and thus we can conclude from Figure 6 that the morphological state of Vectra A900 varied during the experiment which lasted about 2 h..

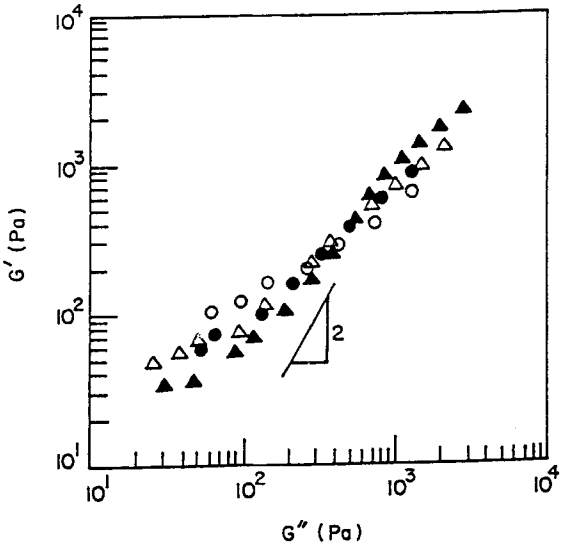

FIGURE 6 Plots of log G' versus log G" for a Vectra A900 specimen having the thermal histories as indicated in the temperature protocol of Figure 5: (O) step 2; (Δ) step 3; (●) step 4; (▲) step 5.

PSHQ10. Figure 7 describes variations of G' and G" with time up to 6 h at a fixed angular frequency $\omega = 0.237$ rad/s for as-cast PSHQ10-A specimens at various annealing temperatures, 130, 135, 140, and 145 °C. Strain amplitude of 0.05 was used to obtain the results given in Figure 7. Note that each measurement lasted about 50 s, and a fresh specimen was used for each test. It can be seen in Figure 7 that for the annealing period of up to 6 h, values of G' and G" at 130, 135, and 140 °C, respectively, increase with annealing time, the rate of increase being faster as the annealing temperature is decreased from 140 to 130 °C, whereas values of G' and G" at 145 °C decrease initially and then remain more or less constant as annealing progresses. It should be remembered that PSHQ10 has the T_{NI} of 175 °C.

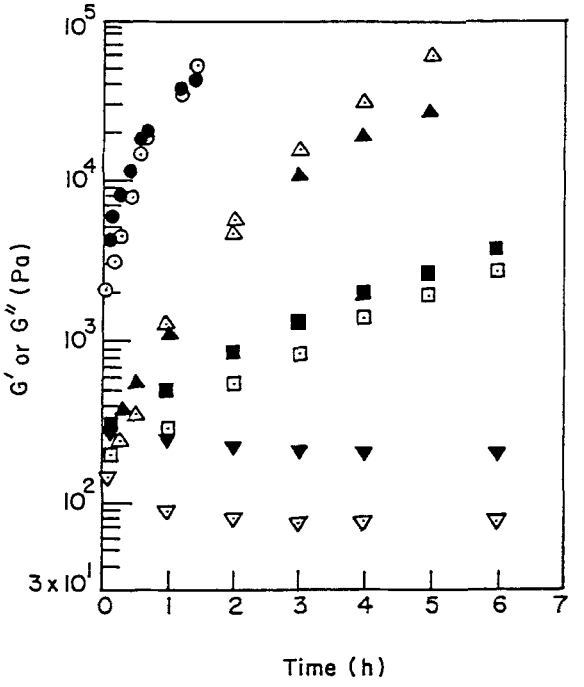

FIGURE 7 Variations of G' (open symbols) and G"(filled symbols) with time for solvent-cast PSHQ10-A during isothermal annealing at various temperatures: (⊙, ●) 130 °C; (△, ▲) 135 °C; (⊡, ■) 140 °C; (▽, ▼) 145 °C. Small amplitude oscillatory deformations with strain amplitude of 0.05 and angular frequency of 0.237 rad/s were applied to the specimens. A fresh specimen was used for each run .

Figure 8 describes variations of complex viscosity $|\eta^*|$ (⊡) with time up to 50 h for an as-cast PSHQ10-A specimen, which was first placed in the cone-and-plate fixture at 190 °C (i.e., at the *isotropic* state), sheared at $\dot{\gamma} = 0.085\ s^{-1}$ for 5 min, and then cooled slowly down to 130 °C. Also given in Figure 8 are, for comparison, variations of $|\eta^*|$ (⊙) with time for an as-cast PSHQ10-A specimen at 130 °C, which was placed in the cone-and-plate fixture preheated at 130 °C. It can be seen in Figure 8 that values of $|\eta^*|$ for the specimen, which had received thermal treatment at 190 °C, are more or less constant for over 50 h tested. The difference in the variation of $|\eta^*|$ with time between the two specimens, one *with* thermal treatment at the *isotropic* state and the other *without* thermal treatment, can be explained with the aid of DSC traces given

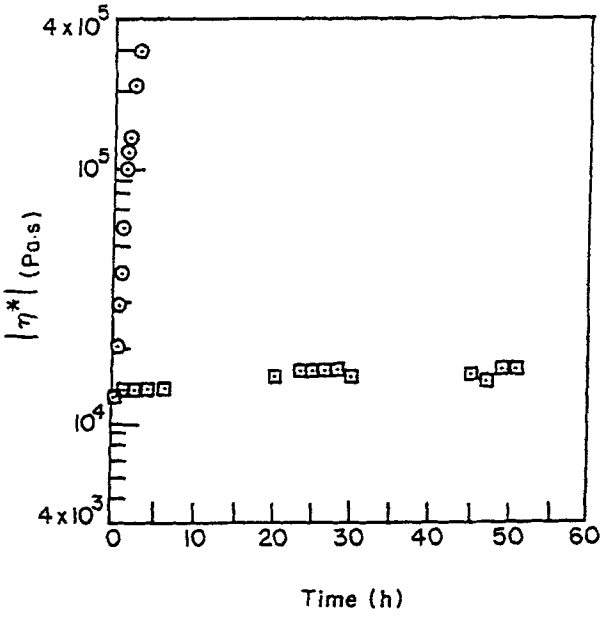

FIGURE 8 Variations of $|\eta^*|$ with time during annealing at 130 °C for two as-cast PSHQ10-A specimens having the following thermal histories: (⊙) an as-cast specimen placed in the cone-and-plate fixture preheated at 130 °C; (⊡) an as-cast specimen placed in the cone-and-plate fixture preheated at 190 °C, subjected to steady shear flow at $\dot{\gamma} = 0.085\ s^{-1}$ for 5 min at 190 °C, and then cooled slowly down to 130 °C. Small amplitude oscillatory deformations with strain amplitude of 0.05 and angular frequency of 0.237 rad/s were applied to the specimens. A fresh specimen was used for each run.

in Figures 9 and 10. Specifically, Figure 9 describes that when an as-cast PSHQ10-A specimen was annealed at 130 °C, it exhibits two endothermic peaks at temperatures above its melting point (115 °C). But, when an as-cast PSHQ10-A specimen first received thermal treatment at the *isotropic* state and was then annealed at 130 °C, as shown in Figure 10, only one endothermic peak at 170-177 °C, which represents T_{NI}, appears. We thus conclude that the rapid increase of G' and G" with time at 130 °C observed in Figure 7, and the rapid increase of $|\eta^*|$ with time at 130 °C observed in Figure 8, are attributable to the presence of a low-melting 'crystal-like' phase,[16] giving rise to an endothermic peak at a temperature between T_m and T_{NI} (see Figure 9).

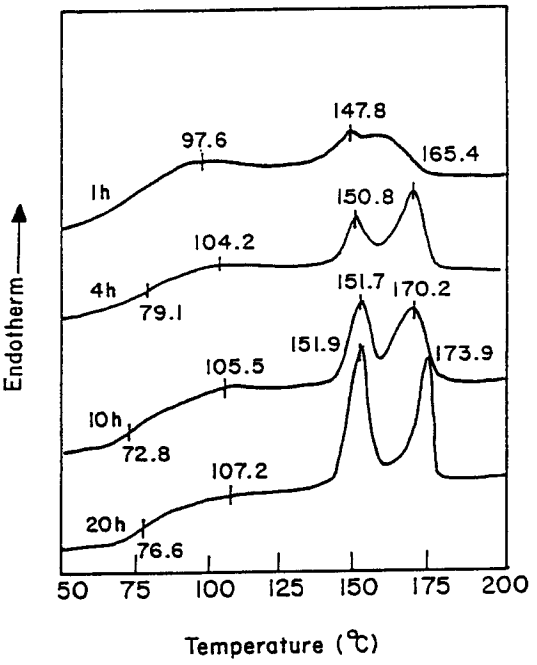

FIGURE 9 DSC traces for as-cast PSHQ10-A specimens annealed at 130 °C for different periods, as indicated on the plot. A fresh specimen was used for each run and the heating rate was 20 °C/min.

Research is in progress to determine the structure of the 'crystal-like' phase using wide-angle X-ray diffraction.

Effect of Thermal History on the Transient and Steady Shear Flow Behaviors

Vectra A900. Transient and steady shear flow behaviors were investigated for Vectra A900. In the light of the disagreement between the results of Guskey and Winter[10] and of Cocchini et al.,[11] emphasis was placed on investigating the effects of (a) the waiting period between the completion of sample loading and the initiation of shear flow and (b) applied shear rate. In the experiments reported below using Vectra A900, we followed very closely the sample loading procedure described in a paper by Guskey and Winter,[10] namely, (1) a compression-molded specimen was inserted in the cone-and-plate fixture which was preheated to 320 °C; (2) after waiting for 1 min at 320 °C to melt away HBA, the temperature was first lowered to 310 °C, which took about 1 min, and then

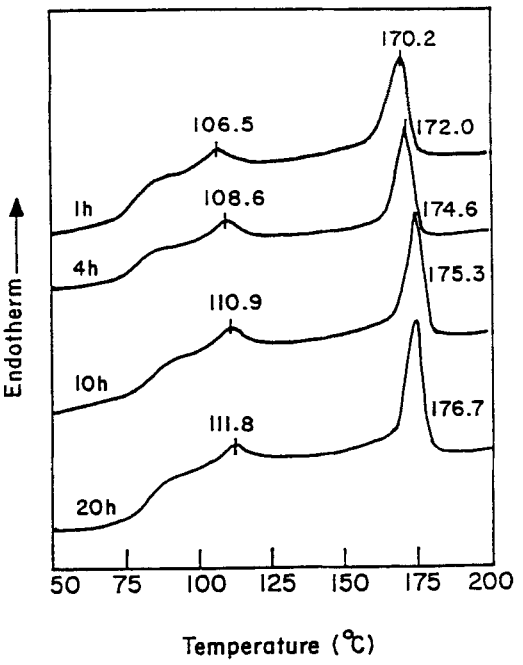

FIGURE 10 DSC traces for as-cast PSHQ10 specimens annealed at 130 °C for different periods, as indicated on the plot, having the following thermal histories: an as-cast specimen was first annealed at 130 °C for 30 min, then heated to 190 °C and held there for 30 min, and finally cooled down slowly to 130 °C for further annealing. A fresh specimen was used for each run and the heating rate was 20 °C/min.

the specimen of about 2 mm (or 1 mm) in thickness was squeezed down to the gap setting of 50 μm and the edge of the specimen was trimmed. This process took about 5 min; (3) the temperature of the specimen was further lowered to 290 °C, which took about 5 min; (4) we waited for about 5 min for temperature equilibration before a sudden shear flow was applied to the specimen. We also varied the waiting period after the temperature equilibration at 290 °C, the reason of which will become clear below when presenting the trace of normal stress signals during the experiment.

Figure 11 gives the trace of normal stress for a Vectra A900 specimen from the time of specimen loading at 320 °C to the end of steady shear flow at 290 °C at $\dot{\gamma} = 0.05\ s^{-1}$.

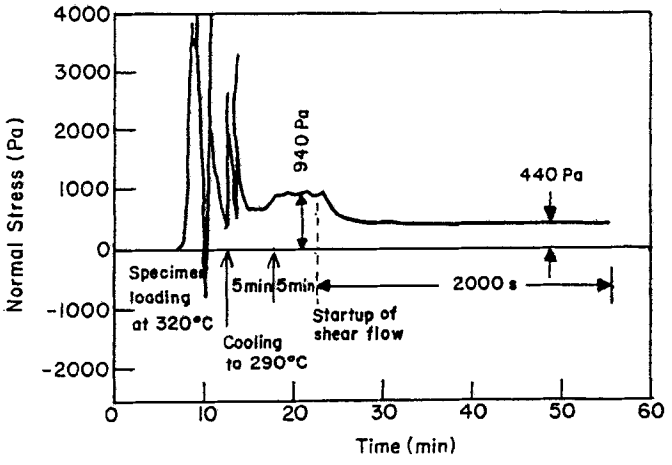

FIGURE 11 Trace of normal stress for Vectra A900: (a) during sample loading at 320 °C; (b) during squeezing and cooling to 290 °C; (c) during temperature equilibration at 290 °C for 5 min; (d) transient and steady shear flows at $\dot{\gamma} = 0.05\ s^{-1}$ for 2000 s; and (e) during relaxation after cessation of shear flow. An unrelaxed normal stress of 940 Pa was present in the specimen before being subjected to shear flow.

Notice in Figure 11 that at the end of the 5 min waiting period at 290 °C a considerable amount of *unrelaxed* normal stress (ca. 940 Pa) remained in the specimen. It should be mentioned that the normal stress was introduced by the squeeze flow during sample loading, reducing the distance between the tip of the cone and plate from 2 mm (sample thickness) to 50 μm. It can be seen in Figure 11 that upon applying a sudden shear flow to the specimen, the normal stress exhibits a very small overshoot and then decreases to a constant value, which is lower than the *unrelaxed* normal stress that existed in the specimen just before being subjected to a sudden shear flow, but much higher than the *true* zero level, as determined before the specimen loading.

Figure 12 gives the trace of normal stress for a Vectra A900 specimen, which was sheared at $\dot{\gamma} = 0.5\ s^{-1}$ for 200 s after waiting for 25 min upon temperature equilibration at 290 °C. It can be seen in Figure 12 that the specimen had the *unrelaxed* normal stress of 860 Pa, which is lower than the value (960 Pa) observed after waiting for only 5 min

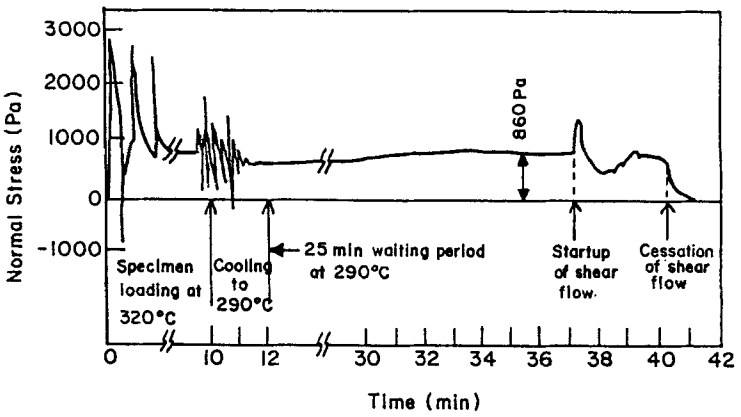

FIGURE 12 Trace of normal stress for Vectra A900: (a) during sample loading at 320 °C; (b) during squeezing and cooling to 290 °C; (c) during temperature equilibration at 290 °C for 25 min; (d) transient and steady shear flows at $\dot{\gamma} = 0.5\ s^{-1}$ for 200 s; and (e) during relaxation after cessation of shear flow. An unrelaxed normal stress of 860 Pa was present in the specimen before being subjected to shear flow.

(see Figure 11). Notice in Figure 12 that, upon startup of shear flow, the normal stress first goes through a rather large maximum and also a minimum and, finally, it tends to level off at the end of shearing for 200 s. The duration of shearing for 200 s was chosen in order to have the same shear strain ($\dot{\gamma}t$) of 100 as in other experimental runs having different shear rates. The following two observations are worth noting in Figure 12: (1) the normal stress at the end of shearing for 200 s (i.e., just before the cessation of shear flow) is smaller than the *unrelaxed* normal stress that existed in the specimen just before being subjected to a sudden shear flow, but much larger than the *true* zero level, and (2) after cessation of shear flow, the normal stress relaxes, approaching *true* zero level (i.e., baseline).

In order to test whether or not the normal stress, which had been introduced by the squeeze flow during sample loading, might be relaxed further if waited for a longer period, we waited for 4 h after the sample loading and the trace of normal stress from the experiment is given in Figure 13. It can be seen in Figure 13 that the *unrelaxed* normal stress for Vectra A900 decreased to 195 Pa after waiting for 4 h upon completion of sample loading and after temperature equilibration at 290 °C. We can

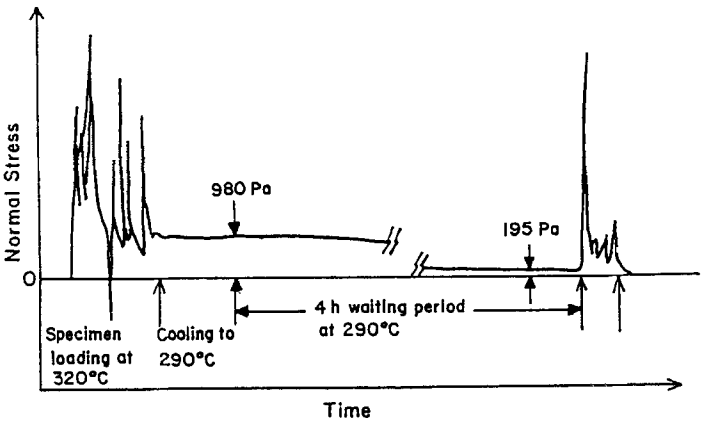

FIGURE 13 Trace of normal stress for Vectra A900: (a) during sample loading at 320 °C; (b) during squeezing and cooling to 290 °C; (c)during temperature equilibration at 290 °C for 4 h; (d) transient and steady shear flows at $\dot{\gamma} = 0.5\ s^{-1}$ for 200 s; and (e) during relaxation after cessation of shear flow. An unrelaxed normal stress of 940 Pa was present in the specimen before being subjected to shear flow.

conclude from Figures 11-13 that the *unrelaxed* normal stress, which was introduced by the squeeze flow during specimen loading, decreases with increasing waiting time under a quiescent isothermal condition. This observation is consistent with that reported earlier by Cocchini et al.[20] Notice in Figure 13 that (a) upon applying a sudden shear flow at $\dot{\gamma} = 0.5\ s^{-1}$, the normal stress exhibits a *very large* overshoot and normal stress of the specimen relaxes to zero value after cessation of shear, which is consistent with that given in Figure 12. Later in this paper we shall elaborate on the reason(s) why such a huge overshoot in normal stress is observed in Figure 13.

Figure 14 gives plots of the first normal stress difference growth $N_1^+(t,\dot{\gamma})$ versus shear strain $\dot{\gamma}t$ for Vectra A900 specimens at 290 °C, in which the *true* zero level of normal stress is taken as the reference value. It should be mentioned that the experimental runs at three different applied shear rates, given in Figure 14, were made by waiting for 5 min after temperature equilibration at 290 °C. Notice in Figure 14 that at $\dot{\gamma}t = 0$ the initial value of N_1 was: (a) 940 Pa when sheared at $\dot{\gamma} = 0.05\ s^{-1}$, (b) 1060 Pa when sheared at $\dot{\gamma} = 0.1\ s^{-1}$, and (c) 923 Pa when sheared at $\dot{\gamma} = 0.3\ s^{-1}$. Theoretically, the initial value of N_1 should be the same in all three runs because the waiting

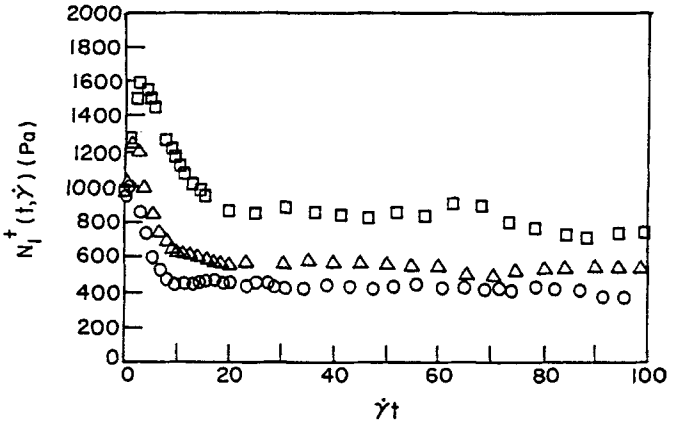

FIGURE 14 Plots of $N_1^+(t,\dot{\gamma})$ versus $\dot{\gamma}t$ for Vectra A900 at 290 °C for various shear rates: (O) 0.05 s^{-1}; (Δ) 0.1 s^{-1}; ($\square$) 0.3 s^{-1}. A fresh specimen was used for each applied shear rate. Each specimen, after being cooled from 320 °C to 290 °C, was annealed for 5 min before being subjected to shear flow. The *unrelaxed* normal stress present in the specimens (i.e., the value of $N_1^+(t=0,\dot{\gamma})$) was 940 Pa for the run at 0.05 s^{-1}, 1060 Pa for the run at 0.1 s^{-1}, and 923 Pa for the run at 0.3 s^{-1}.

period upon completion of sample loading was the same, 5 min. This points out the real difficulty in controlling the initial condition of the specimen, because the physical squeezing of a specimen placed in the cone-and-plate fixture, however careful one might be, is hard to reproduce, thus giving rise to variations in the amount of normal stress introduced during sample loading. We observed from Figure 14 that values of N_1 for Vectra A900 are *positive*. However, information in Figure 14 is of *little* rheological significance, because rheological measurement for each run was made under the condition where a substantial amount of *unrelaxed* normal stress was present in the specimen before being subjected to startup shear flow.

Figure 15 gives plots of shear stress growth $\sigma^+(t,\dot{\gamma})$ versus $\dot{\gamma}t$ for Vectra A900 specimens at 290 °C for three different values of applied shear rate. During the experiment we observed that shear stress was zero after completion of sample loading and during temperature equilibration at 290 °C. Therefore the value of $\sigma^+(t,\dot{\gamma})$ starts from *zero* upon startup of shear flow. It can be seen in Figure 15 that a very large overshoot

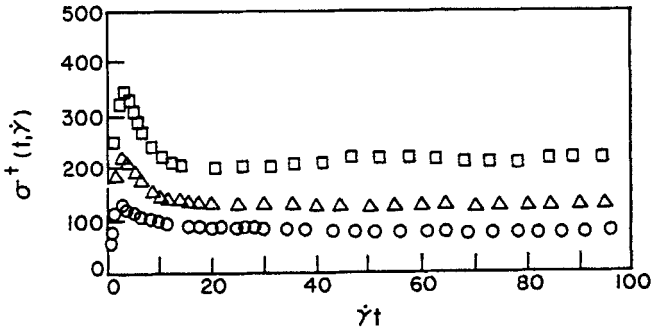

FIGURE 15 Plots of $\sigma^+(t,\dot{\gamma})$ versus $\dot{\gamma}t$ for Vectra A900 at 290 °C for various shear rates: (O) 0.05 s^{-1}; (Δ) 0.1 s^{-1}; (□) 0.3 s^{-1}. The thermal histories of the specimens are identical with those given in Figure 14.

occurs in $\sigma^+(t,\dot{\gamma})$, the magnitude of which increased with increasing applied shear rate. The display of such a large value of overshoot in Figure 15 is attributable to the breakup of polydomains in the specimen.

When the normal stress data given in Figure 14 are plotted against $\dot{\gamma}t$ by neglecting the *unrelaxed* normal stress that was actually present in the specimen before being subjected to startup of shear flow, we obtain the results given in Figure 16, indicating that values of N_1 are *negative* at low shear rates. This observation is consistent with that made earlier by Guskey and Winter.[10] It should be remembered, however, as given in Figure 11, that a considerable amount of *unrelaxed* normal stress existed in the specimen before being subjected to a sudden shear flow when we waited for *only* 5 min after temperature equilibration at 290 °C. We thus conclude that an erroneous interpretation of the normal stress behavior of Vectra A900 can be made *if* one neglects the presence of *unrelaxed* normal stress in the specimen. This is how Guskey and Winter[10] reported *negative* values of N_1 for Vectra A900 at 290 °C, which we believe is not correct.

It should be mentioned that we found, within experimental uncertainties, the specimen of 1 mm initial thickness gave rise to virtually the same amount of *unrelaxed* normal stress, after waiting for 5 min upon completion of specimen loading and temperature equilibration at 290 °C, as the specimen of 2 mm initial thickness. This is understandable in that, the distance that the upper plate of the cone-and-plate fixture had

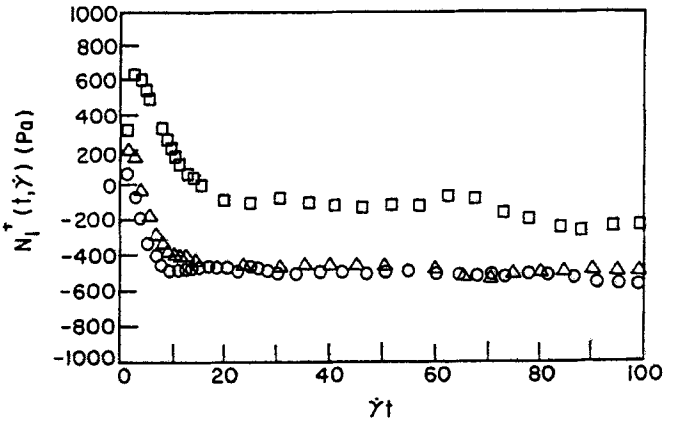

FIGURE 16 Plots of $N_1^+(t,\dot{\gamma})$ versus $\dot{\gamma}t$ for Vectra A900 at 290 °C for various shear rates: (O) 0.05 s^{-1}; (Δ) 0.1 s^{-1}; (□) 0.3 s^{-1}, which were obtained by assuming that there was *no* unrelaxed normal stress in specimen, i.e., $N_1^+(t=0,\dot{\gamma})$ was assumed to be zero, which certainly is not true. Otherwise the thermal histories of the specimens are the same as in Figure 14.

to travel during sample loading was so large, that either the travel from 1 mm to 50 μm or from 2 mm to 50 μm apparently did not make any discernible difference insofar as the amounts of the *unrelaxed* normal stress generated by the squeeze flow during specimen loading was concerned.

When a Vectra A900 specimen was sheared at $\dot{\gamma} = 0.5\ s^{-1}$ we observed evidence of the onset of flow instability. Specifically, we observe from Figure 17 that upon applying a sudden shear flow at $\dot{\gamma} = 0.5\ s^{-1}$ after temperature equilibration at 290 °C for 5 min, the specimen exhibits a very large overshoot in normal stress and then irregularities in normal stress, signifying that flow instability set in after shearing for about 120 s. Figure 18 gives the enlarged trace of the normal stress signal during the shear flow, showing a sudden dip at a shear strain of about 60 and then another maximum in normal stress, the magnitude of which being even greater than the magnitude of the previous peak. Without encountering flow instability, there is no reason why the peak value of normal stress in the third cycle can become greater than that of the second cycle.

Let us now return to Figure 13, showing the trace of normal stress of the Vectra

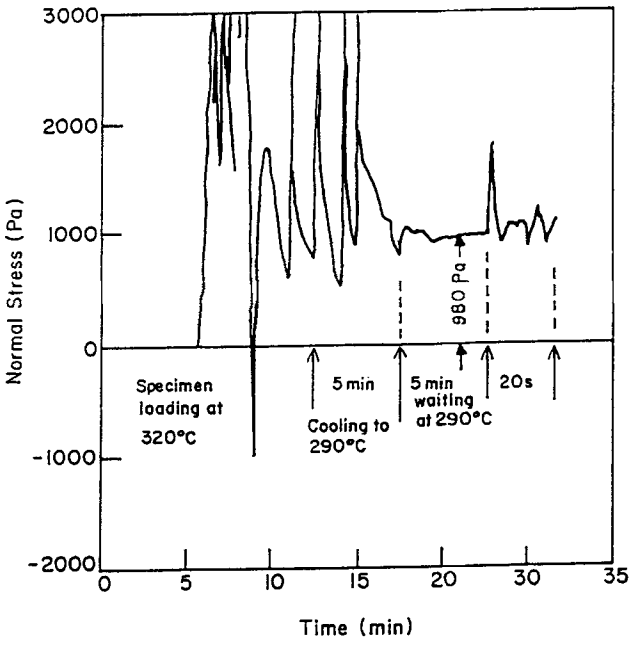

FIGURE 17 Trace of normal stress for Vectra A900: (a) during sample loading at 320 °C; (b) during squeezing and cooling to 290 °C; (c) during temperature equilibration at 290 °C for 5 min; and (d) transient and steady shear flows at $\dot{\gamma} = 0.5\ s^{-1}$ for 200 s. An unrelaxed normal stress of 980 Pa was present in the specimen before being subjected to a sudden shear flow.

A900 specimen which had been annealed for 4 h in the cone-and-plate fixture before being subjected to startup shear flow. In order to facilitate our discussion here, the trace of $N_1^+(t,\dot{\gamma})$ versus $\dot{\gamma}t$ is given in Figure 19, showing that a very large overshoot in $N_1^+(t,\dot{\gamma})$ occurs right after the startup of shear flow, followed by irregularities in $N_1^+(t,\dot{\gamma})$, which signifies the occurrence of flow instability. It is of interest to observe that the peak value of $N_1^+(t,\dot{\gamma})$ for the specimen which was annealed for 4 h (see Figure 19) is about 5100 Pa, which is about 2.5 times the peak value of $N_1^+(t,\dot{\gamma})$ for the specimen which was annealed only for 5 min (see Figure 18). This difference can be explained with the aid of Figure 20, which indicates that the rheological behavior (thus the morphological state of the specimen) after annealing for 4 h is quite different from that after annealing for *only* 5 min. It should be mentioned that Figure 20 was obtained

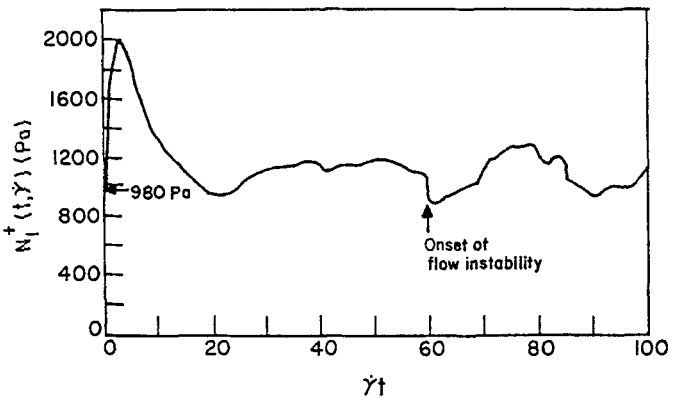

FIGURE 18 Plot of $N_1^+(t,\dot{\gamma})$ versus $\dot{\gamma}t$ for Vectra A900 at 290 °C for $\dot{\gamma}$ = 0.5 s^{-1}, where the thermal history of the specimen is the same as in Figure 17 and $N_1^+(t=0,\dot{\gamma})$ = 980 Pa. The arrow indicates the onset of flow instability.

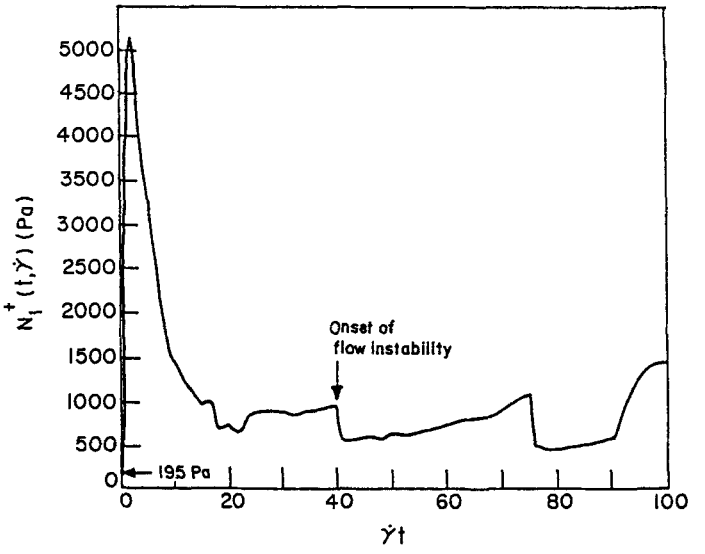

FIGURE 19 Plot of $N_1^+(t,\dot{\gamma})$ versus $\dot{\gamma}t$ for Vectra A900 at 290 °C for $\dot{\gamma}$ = 0.5 s^{-1}, where the thermal history of the specimen is the same as in Figure 13 and $N_1^+(t=0,\dot{\gamma})$ = 195 Pa. The arrow indicates the onset of flow instability.

by applying small amplitude oscillatory deformations, at predetermined time intervals, to a specimen over a period of 4 h, and that the specimen was first heated to 320 °C for 1 min and then cooled down to 290 °C before small amplitude oscillatory deformations were applied. It can be seen in Figure 20 that the rheological properties remained constant for about 1 h and then they increased with further annealing. The reasons for such behavior are not well understood at the present time, although two different explanations can be offered, namely, (a) post polymerization might occur and (b) structural changes might occur during annealing times larger than 1 h.

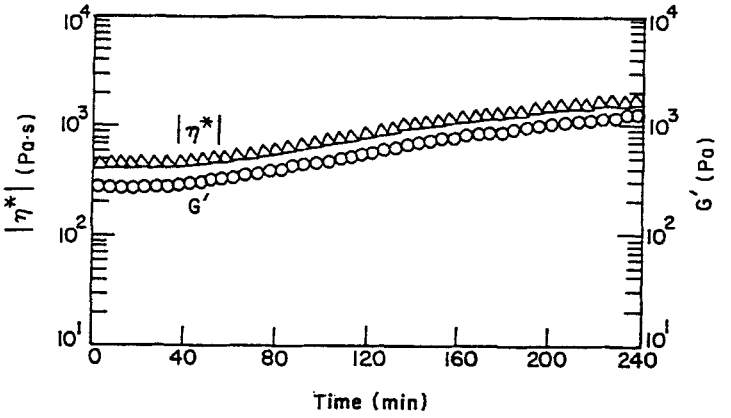

FIGURE 20 Variations of G' and $|\eta^*|$ with time for a Vectra A900 specimen, which was placed in the cone-and-plate fixture at 290 °C, heated to 320 °C for 1 min, and then cooled down to 290 °C followed by annealing for 4 h. Small amplitude oscillatory deformations with strain amplitude of 0.05 and angular frequency of 1 rad/s were applied to the specimen.

PSHQ10. It is very clear from the results presented above that it is important to control the initial conditions before shear flow is applied to a TLCP in an *aniostropic* state. In order to observe whether or not the initial conditions of PSHQ10 in the *nematic* state can be controlled, before conducting transient shear flow experiments we conducted frequency sweep experiments using a specimen having the following temperature protocols: (1) an as-cast specimen was first placed in the cone-and-plate fixture preheated at 190 °C in the *isotropic* state and then a frequency sweep experiment was conducted (step 1); (2) the specimen was cooled down to 140 °C and then a

frequency sweep experiment was conducted (step 2); (3) the specimen was heated back to 190 °C and a frequency sweep experiment was conducted (step 3); (4) the specimen was once again cooled down to 140 °C and then a frequency sweep experiment was conducted (step 4); and (5) the specimen was heated back once again to 190 °C and a frequency sweep experiment was conducted (step 5). The thermal history of the specimen is summarized in the upper panel of Figure 21, and the results of the frequency sweep experiments are given in terms of log G' versus log G" plots in the lower panel of Figure 21

It can be seen in Figure 21 that three repeated measurements at 190 °C in the *isotropic* state give rise to a single correlation and two repeated measurements at 140 °C in the *nematic* state give rise to a single correlation for PSHQ10-B. Notice in Figure 21 that the log G' versus log G" plot in the *nematic* state lies above that in the *isotropic* state, reflecting the difference in the morphological state of the polymer at the two different temperatures. It should be mentioned that the entire experiment summarized in Figure 21 lasted over 4 h. A comparison of Figure 21 with Figure 6 reveals that the rheological measurements for PSHQ10-B at 140 °C were reproducible for a period of over 4 h, whereas the rheological measurements for Vectra A900 at 290 °C were *not* reproducible for a period of 2 h. The significance of Figure 21 lies in that the initial conditions (i.e., initial morphology) of PSHQ10-B can be controlled by first heating an as-cast specimen to the *isotropic* state and then cooling slowly down to a preset temperature in the *nematic* state.

We will show below that the experimental difficulties with Vectra A900 described above can be eliminated entirely in the use of PSHQ10. Figure 22 gives the trace of normal stress for PSHQ10-B specimen from the instant of specimen loading in the cone-and-plate fixture at 190 °C to the end of steady shear flow at 160 °C for $\dot{\gamma} = 0.1$ s^{-1}. The following temperature protocols were used: (a) first, an as-cast PSHQ10-B specimen was placed in the cone-and-plate fixture which had been preheated to 190 °C, which is 15 °C above the T_{NI} of PSHQ10; (b) after the temperature was equilibrated at 190 °C, the gap setting was adjusted from about 2 mm (the specimen thickness) to 160 μm by applying squeeze flow and the excess material was trimmed off. The entire process took about 20 min. Then the temperature of the specimen was lowered from 190 to 160 °C, which took about 25 min; (c) after temperature equilibration at 160 °C for 5 min, a sudden shear flow was applied to the specimen. It is significant to note in Figure 22 that just before the startup of shear flow, the normal stress was *zero*, which was the baseline as determined before sample loading; (d) upon startup of shear flow,

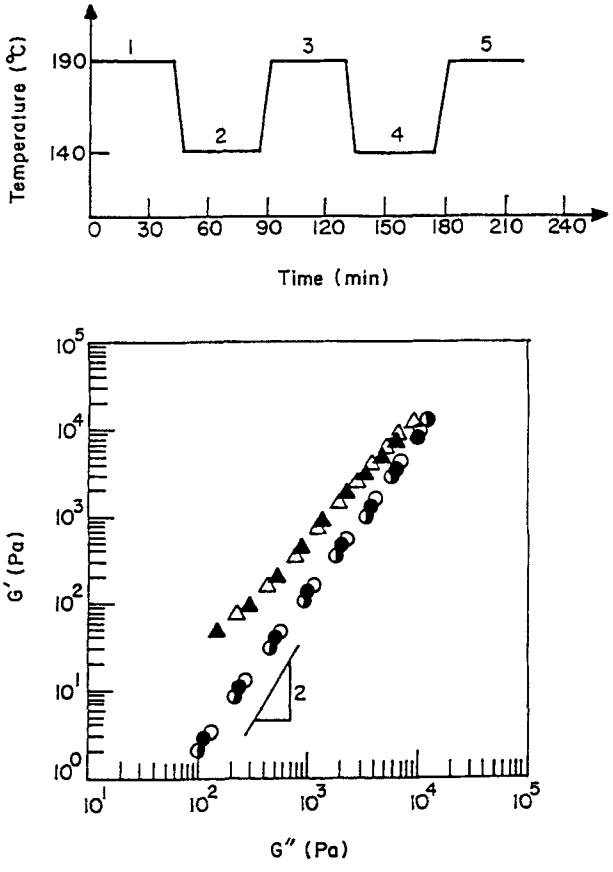

FIGURE 21 Temperature protocol employed and plots of log G' versus log G" for a PSHQ10-B specimen having the thermal histories as indicated in the temperature protocol: (○) step 1; (△) step 2; (◑) step 3; (▲) step 4; (●) step 5.

the normal stress goes through a large maximum (exceeding the limit of the setting of the chart recorder) followed by a mild peak and then finally leveled off to a constant value; (e) upon cessation of steady shear flow, the normal stress decreased rapidly to *zero*, which was the baseline as determined before sample loading.

Figure 23 gives a typical trace of normal stress, showing variations of $N_1^+(t,\dot{\gamma})$ for a PSHQ10-B specimen at 160 °C during the transient and steady shear flow at $\dot{\gamma} = 0.1\ s^{-1}$. Notice in Figure 23 that $N_1^+(t,\dot{\gamma})$ goes through a very sharp minimum, exhibiting

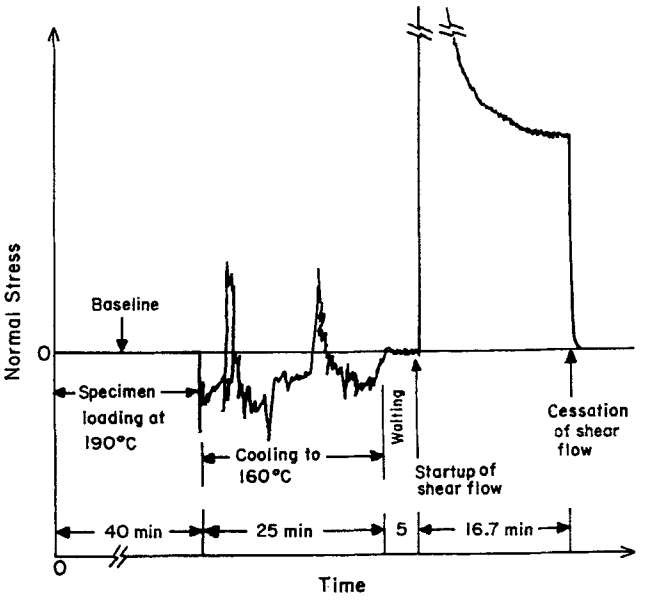

FIGURE 22 Trace of normal stress for a PSHQ10-B specimen: (a) during sample loading at 190 °C; (b) during squeezing and cooling to 160 °C; (c) during temperature equilibration at 160 °C for 5 min; (d) transient and steady shear flows at $\dot{\gamma} = 0.1\ s^{-1}$ for 2000 s; and (e) during relaxation after cessation of shear flow. The normal stress of the specimen before being subjected to shear flow is zero, which is the baseline as determined before specimen loading.

transient *negative* values of $N_1^+(t,\dot{\gamma})$, followed by a very large maximum and then levels off to a constant value.

By employing the temperature protocols described above in reference to Figure 22, we conducted a series of startup and steady shear flow experiments at different temperatures for a fixed applied shear rate, and at different applied shear rates for a fixed temperature. The effect of temperature on the shear stress growth $\sigma^+(t,\dot{\gamma})$ of PSHQ10-A is given in Figure 24 at $\dot{\gamma} = 0.536\ s^{-1}$ for 130, 140, and 150 °C. An inset is given in Figure 24, in order to observe how the value of $\dot{\gamma}t$ at which a maximum in $\sigma^+(t,\dot{\gamma})$ appears varies with measurement temperature. It can be seen in Figure 24 that the $\dot{\gamma}t$ at which a maximum in $\sigma^+(t,\dot{\gamma})$ appears tends to shift to a larger value as the

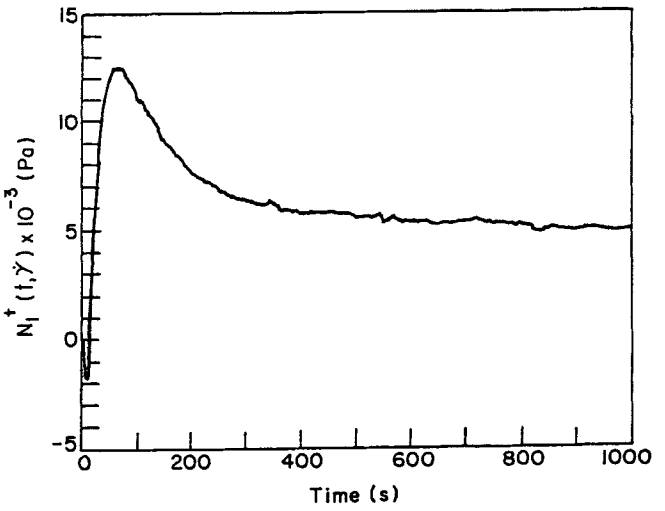

FIGURE 23 Trace of $N_1^+(t,\dot{\gamma})$ for a PSHQ10-B specimen at 160 °C during the startup shear flow at $\dot{\gamma} = 0.1\ s^{-1}$, where the thermal history of the specimen is the same as in Figure 22.

temperature decreases, and the value of maximum $\sigma^+(t,\dot{\gamma})$ becomes greater as the temperature decreases. These observations seem to suggest that as the temperature of PSHQ10 moves farther below the T_{NI}, greater shear stresses are required to break up polydomains, which were present in the specimen before being subjected to a sudden shear flow.

The effect of temperature on the $N_1^+(t,\dot{\gamma})$ of PSHQ10-A is given in Figure 25 at $\dot{\gamma} = 0.536\ s^{-1}$ for 130, 140, and 150 °C. It can be seen in Figure 25 that multiple peaks in $N_1^+(t,\dot{\gamma})$ appear at all three temperatures tested and the magnitude of the $N_1^+(t,\dot{\gamma})$ maximum increases with decreasing temperature. From Figure 25 we conclude that the temperature (thus the initial morphology) of a PSHQ10 specimen has a profound influence on the transient first normal stress difference. It should be emphasized once again that before being subjected to startup shear flow, the normal stress of the specimen was *zero* at each test temperature in the *nematic* state. We thus conclude that the differences observed in Figures 24 and 25 truly reflect the effect of different temperatures on the specimens. Needless to say, the morphological state of the specimen varies with temperature, which is also reflected in the log G' versus log G" plots.[17]

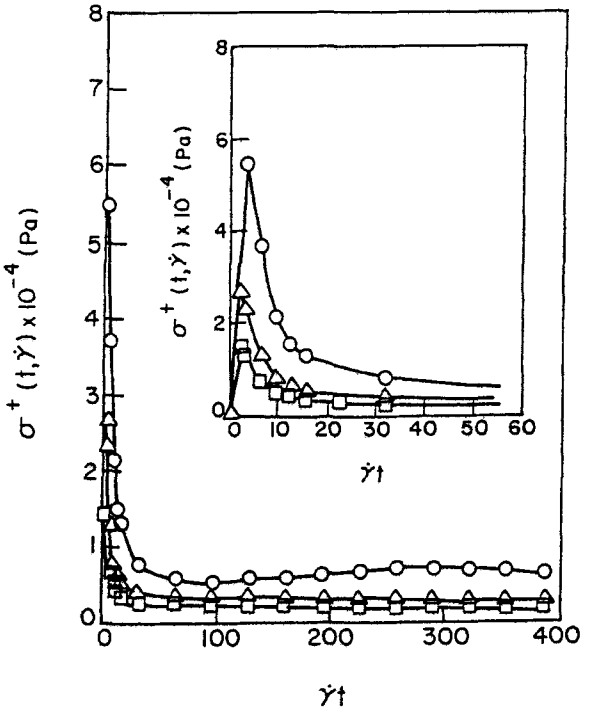

FIGURE 24 Plots of $\sigma^+(t,\dot\gamma)$ versus $\dot\gamma t$ for PSHQ10-A at $\dot\gamma = 0.536\ s^{-1}$ for various temperatures: (O) 130 °C; (Δ) 140 °C; (□) 150 °C. A fresh specimen was used for each temperature, and each specimen received thermal treatment in the isotopic region at 190 °C.

Effect of Preshear on the Steady Shear Flow Properties

Vectra A900. We investigated the effect of preshear on the rheological behavior of Vectra A900 during a subsequent (intermittent or interrupted) shear flow. Figure 26 gives a typical result, showing (a) temperature protocol employed, (b) variations of normal stress from the time of specimen loading to the end of the intermittent shear flow, and (c) the duration of applied shear flow at a rate of 0.1 s^{-1}. Notice in Figure 26 that at the end of the *first* steady shear flow for 16.7 min, the specimen was heated to 320 °C and then cooled down to 290 °C again, and after waiting for 5 min for temperature equilibration the specimen was subjected to the second (intermittent) shear flow at a rate of 0.1 s^{-1} for 16.7 min. As noted in Figure 26, during the intermittent shear flow at 290 °C we observed evidence of the onset of flow instability, showing a

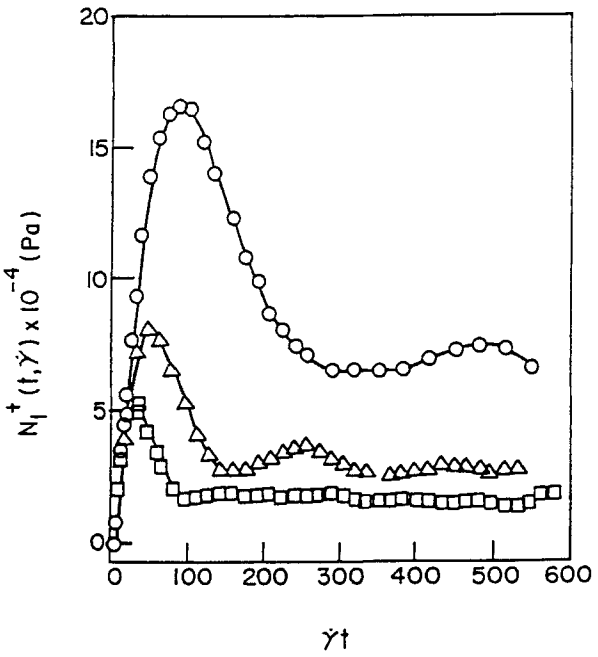

FIGURE 25 Plots of $N_1^+(t,\dot{\gamma})$ versus $\dot{\gamma}t$ for PSHQ10-A at $\dot{\gamma} = 0.536\ s^{-1}$ for various temperatures: (O) 130 °C; (Δ) 140 °C; (□) 150 °C. A fresh specimen was used for each temperature, and each specimen received thermal treatment in the isotopic region at 190 °C.

sudden dip of normal stress to virtually the baseline.

The following observations are worth noting in Figure 26: (1) when the specimen was cooled from 320 to 290 °C for the first time and after temperature equilibration for 5 min at 290 °C, the amount of *unrelaxed* normal stress in the specimen before being subjected to the *first* startup shear flow was 880 Pa; (2) but when the specimen was heated to 320 °C once again at the end of the *first* shear flow experiment and then cooled down to 290 °C for the second time, the amount of *unrelaxed* normal stress was 520 Pa. Figure 27 gives the traces of $N_1^+(t,\dot{\gamma})$ for Vectra A900 in the *first* (*initial*) and *second* (*intermittent*) transient shear flow experiments. It can be seen in Figure 27 that the level of steady-state first normal stress difference (N_1) is decreased from 420 Pa in the *initial* shear flow experiment to 290 Pa in the *intermittent* shear flow experiment. In

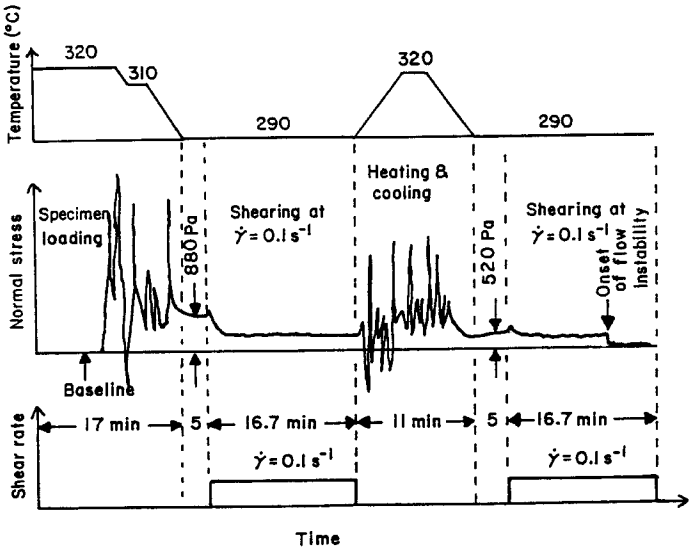

FIGURE 26 Temperature protocol employed, variations of normal stress with time for Vectra A900 during the *first* and *second* startup shear flows at $\dot{\gamma} = 0.1\ s^{-1}$, and the duration of applied shear flow. Note that an *unrelaxed* normal stress of 880 Pa was present in the specimen before being subjected to the *first* startup shear flow and an *unrelaxed* normal stress of 520 Pa was present in the *presheared* specimen before being subjected to the *second* startup shear flow. After reaching steady state upon startup of the *first* shear flow, the specimen was heated to 320 °C and cooled down to 290 °C before being subjected to the *second* (intermittent) shear flow.

other words, the *presheared* specimen has smaller values of N_1, as compared to the *unsheared* specimen. This is attributable to the breakup of polydomains during the *first* shearing experiment.

PSHQ10. Figure 28 gives logarithmic plots of steady shear viscosity (η) versus shear rate ($\dot{\gamma}$) for PSHQ10-A at 130, 140, 150, and 160 °C, using *fresh* (*unsheared*) specimens (open symbols) and the specimens which already had been *presheared* from 0.0085 to 0.27 s^{-1} (filled symbols). It can be seen in Figure 28 that *preshearing* of a PSHQ10-A specimen decreased the values of η at low shear rates but affected little the

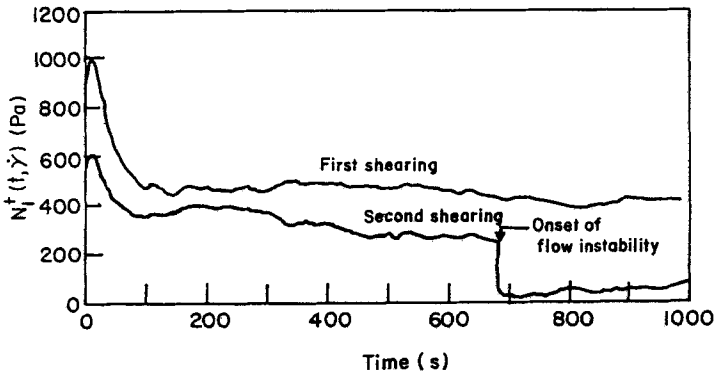

FIGURE 27 Traces of $N_1^+(t,\dot{\gamma})$ for a Vectra A900 specimen at 290 °C during the first startup shear flow and during the intermittent shear flow at $\dot{\gamma} = 0.1\ s^{-1}$, where the thermal history of the specimen is the same as in Figure 26.

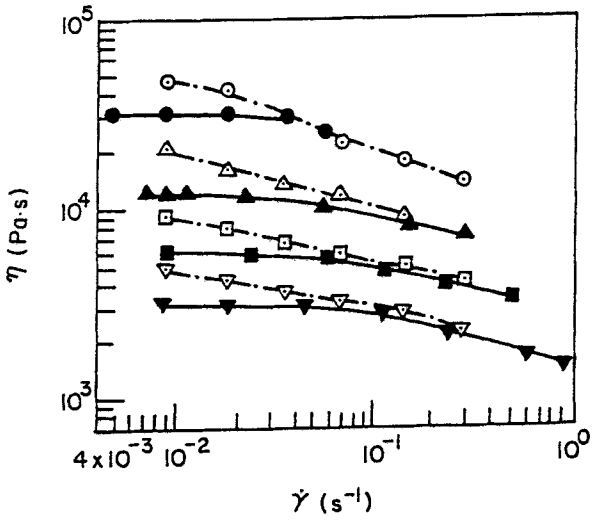

FIGURE 28 (a) Plots of log η versus log $\dot{\gamma}$ (open symbols) for *fresh* PSHQ10-A specimens at various temperatures: (⊙) 130 °C; (Δ) 140 °C; (⊡) 150 °C; (▽) 160 °C; and (b) plots of log η versus log $\dot{\gamma}$ (filled symbols) for *presheared* PSHQ10-A specimens at various temperatures: (●) 130 °C; (▲) 140 °C; (■) 150 °C; (▼) 160 °C. A single specimen was employed for each temperature, and each specimen was *presheared* at rates ranging from 0.0085 to 0.27 s^{-1}.

values of η at higher shear rates. Figure 29 gives plots of log N_1 versus log $\dot{\gamma}$ for fresh (*unsheared*) PSHQ10 specimens (open symbols) and for *presheared* PSHQ10-A specimens (filled symbols) at 130, 140, 150, and 160 °C, showing that *preshearing* decreased the values of N_1 over the range of $\dot{\gamma}$ tested. It can be seen in Figure 29 that *preshearing* also decreased the values of N_1.

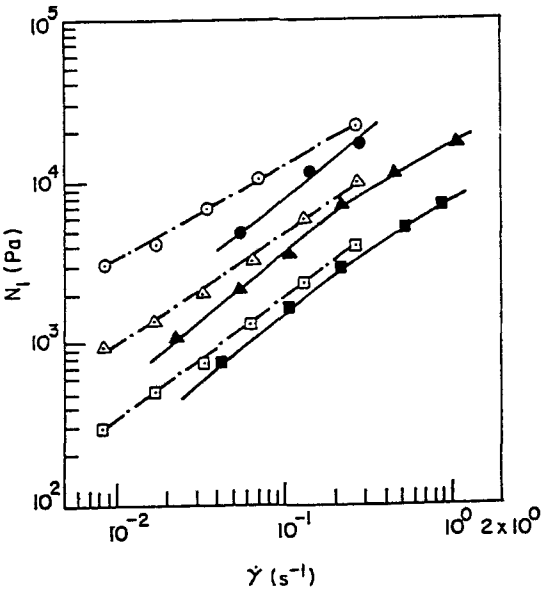

FIGURE 29 (a) Plots of log N_1 versus log $\dot{\gamma}$ (open symbols) for *fresh* PSHQ10-A specimens at various temperatures: (⊙) 140 °C; (Δ) 150 °C; (⊡) 160 °C; and (b) plots of log N_1 versus log $\dot{\gamma}$ (filled symbols) for *presheared* PSHQ10-A specimens at various temperatures: (●) 140 °C; (▲) 150 °C; (■) 160 °C. A single specimen was employed for each temperature, and each specimen was *presheared* at rates ranging from 0.0085 to 0.27 s^{-1}.

CONCLUDING REMARKS

In this study we have investigated the transient, steady-state and oscillatory shear flow behaviors of two TLCPs, Vectra A900 and PSHQ10, using a cone-and-plate rheometer. We have demonstrated that in the use of Vectra A900, the control of initial condition (i.e., initial morphology) is virtually impossible, because the normal stress introduced by

the squeeze flow during sample loading could not be relaxed in a reasonably short by the squeeze flow during sample loading could not be relaxed in a reasonably short period (say, within 1 h). On the other hand, when a Vectra A900 specimen was annealed for a sufficiently long time (say, over 4 h) to relax most of the normal stress that was introduced by the squeeze flow during sample loading, the domain textures of Vectra A900 apparently changed considerably, consequently making an interpretation of the rheological data very difficult. As noted earlier by Cocchini et al.,[11,20] the presence of *unrelaxed* normal stress, which was introduced by the squeeze flow during sample loading, can lead one to erroneously interpret values of first normal stress difference (N_1) to be *negative* at low shear rates below a certain critical value *if* the *unrelaxed* normal stress value were assumed to be the *true* zero value of the normal stress. In this paper we have shown that values of N_1 are *positive* for the range of shear rates, 0.01-1.0 s^{-1}, investigated when the *unrelaxed* normal stress that existed in the specimen at the beginning of the startup of shear flow is properly taken into account.

Because PSHQ10 has a relatively low clearing temperature (175 °C), which is quite below its thermal degradation temperature (350 °C), before taking rheological measurements we were able to erase the thermal history associated with polymerization and sample preparation, by first heating to 190 °C (in the *isotropic* region), shearing there at a low shear rate (0.085 s^{-1}) for 5 min and then cooling slowly down to a preset temperature in the *nematic* region. This procedure enabled us to control the initial morphology of PSHQ10 specimens for rheological measurements. The control of initial morphology is essential to obtain reproducible transient rheological responses for TLCPs, because the initial morphology (in the form of polydomains) of a TLCP greatly affects its rheological responses.

The use of PSHQ10 in the present study relieved us from another potential difficulty in obtaining reliable rheological data during transient shear flow experiments. That is, by placing a PSHQ10 specimen in the cone-and-plate fixture at 190°C (in the *isotropic* region), we did not have to worry about how fast the normal force might decay after a specimen had been loaded. We confirmed that there was *negligible* normal force in the PSHQ10 specimen at the *isotropic* state (i.e., $T > 175$ °C) as well as at the *nematic* state before shear flow was applied to a specimen.

When using a TLCP having a high clearing temperature (e.g., HBA/HNA copolyesters), one sometimes *preshears* the specimen in order to control its initial morphology and thus to obtain reproducible rheological data.[11] In such situations, extreme care must be exercised to interpret the rheological data, because the extent of

the applied shear can influence the domain texture and thus rheological properties of the TLCP.

We wish to emphasize the importance of being able to control the initial condition when investigating experimentally the rheological behavior of TLCP. This is particular important if rheological measurements are to be used for developing a molecular theory. It should be mentioned that currently held molecular theories[31-33] assume that macromolecules consists of rigid rods dispersed in a solution, and that the intermolecular potentials employed in those theories must be either modified or replaced with new ones, which would be suitable for thermotropic LCP. Thus, at present it is not possible to compare the experimental results presented above with currently held molecular theories.

REFERENCES

1. W. J. Jackson and H. F. Kuhfuss, *J. Polym. Sci., Polym. Chem. Ed.*, **14**, 2043 (1976).
2. K. F. Wissbrun, Brit. *Polym. J.*, **13**, 163 (1980).
3. K. F. Wissbrun and A. C. Griffin, J. Polym. Sci., *Polym. Phys. Ed.*, **20**, 1835 (1982).
4. M. Prasadarao, E. M. Pearce, and C. D. Han, *J. Appl. Polym. Sci.*, **27**, 1343 (1982).
5. A. D. Gotsis and D. G. Baird, *J. Rheol.*, **29**, 539 (1985).
6. D. Done and D. G. Baird, *J. Rheol.*, **34**, 749 (1990).
7. S. L. Wunder, S. Ramachandran, S. R. Gochanour, and M. Weinberg, *Macromolecules*, **19**, 1696 (1986).
8. K. F. Wissbrun, G. Kiss, and F. N. Cogswell, *Chem. Eng. Comm.*, **53**, 149 (1987).
9. J. M. Gonzalez, M. E. Munoz, M. Cortazar, A. Santamaria and J. J. Pena, *J. Polym Sci., Part B: Polym. Phys.*, **28**, 1533 (1990).
10. S. M. Guskey and H. H. Winter, *J. Rheol.*, **35**, 1191 (1991).
11. F. Cocchini, M. R. Nobile, and D. Acierno, *J. Rheol.*, **35**, 1171 (1991).
12. P. Driscoll T. Masuda, and K. Fujiwara, *Macromolecules*, **24**, 1567 (1991).
13. T. Masuda, K. Fujiwara, and M. Takahashi, *Inter. Polymer Processing*, **6**, 225 (1991).
14. T. De'Neve, P. Navard, and M. Kleman, *J. Rheol.*, **37**, 515 (1993).
15. F. P. La Mantia and A. Valenza, *Polym. Eng. Sci.*, **29**, 625 (1989).
16. S. S. Kim and C. D. Han, *Macromolecules*, **26**, 3176 (1993).

17. S. S. Kim and C. D. Han, *J. Rheol.*, in press.
18. S. S. Kim and C. D. Han, *Polymer*, in press .
19. S. S. Kim and C. D. Han, *J. Polym. Sci., Part B: Polym. Phys.*, in press.
20. F. Cocchini, M. R. Nobile, and D. Acierno, *J. Rheol.*, **36**, 1307 (1992).
21. A. Furukawa and R. W. Lenz, *Macromol. Chem. Macromol. Symp.*, **2**, 3 (1986).
22. T. G. Lin and H. H. Winter, *Macromolecules*, **21**, 2439 (1988); **24**, 2877 (1991).
23. R. A. Chivers, J. Blackwell, and G. A. Gutierrez, *Polymer*, **25**, 435 (1984).
24. G. D. Butzbach, J. H. Wendorff, and H. J. Zimmermann, *Polymer*, **27**, 1337 (1986).
25. C. D. Han and J. Kim, *J. Polym. Sci., Part B: Polym. Phys.*, **25**, 1741 (1987).
26. C. D. Han, J. Kim, and J. K. Kim, *Macromolecules*, **22**, 383 (1989).
27. C. D. Han, D. M. Baek, and J. K. Kim, *Macromolecules*, **23**, 561 (1990).
28. C. D. Han and K. W. Lem, *Polym. Eng. Rev.*, **2**, 135 (1983).
29. C. D. Han and M. S. Jhon, *J. Appl. Polym. Sci.*, **32**, 3809 (1986).
30. C. D. Han, *J. Appl. Polym. Sci.*, **35**, 167 (1988).
31. G. Marrucci and P. L. Maffettone, *Macromolecules*, **22**, 4076 (1989)
32. G. Marrucci and P. L. Maffettone, *J. Rheol.*, **34**, 1217, 1231 (1990).
33. R. G. Larson, *Macromolecules*, 23, 3983 (1990).